



Evaluation of antileishmanial activity of valproic acid against *Leishmania donovani*: An integrated *in silico* and *in vitro* study

Mohamed A. A. Elbadawi,¹ Mohamed K. A. Awadalla,² Marwa S. S. Osman,^{3,4} Magdi A. Mohamed,^{3*} Mahmoud M. E. Mudawi,^{5,6} Muzamil M. Abdel Hamid,⁷ Malik S. Mohamed,⁸ Mohammed A. Gafar⁸

¹Department of Pharmacology, Faculty of Pharmacy, University of Khartoum, Khartoum 11111, Sudan

²College of Pharmacy, University of Hail, Hail 81451, Saudi Arabia

³Department of Pharmaceutical Chemistry, Faculty of Pharmacy, University of Khartoum, Khartoum 11111, Sudan

⁴Department of Pharmaceutical Chemistry, Faculty of Pharmacy, Ahfad University for Women, Khartoum 11111, Sudan

⁵Department of Pharmacology and Toxicology, Faculty of Pharmacy, Northern Border University, Rafha, Saudi Arabia

⁶Department of Pharmacology, Faculty of Pharmacy, Omdurman Islamic University, Omdurman, Sudan

⁷Department of Parasitology and Medical Entomology, Institute of Endemic Diseases, University of Khartoum, Khartoum 11111, Sudan

⁸Department of Pharmaceutics, Faculty of Pharmacy, University of Khartoum, Khartoum 11111, Sudan

Received: 05-01-2016 / Revised: 18-01-2016 / Accepted: 28-01-2016 / Published: 30-01-2016

ABSTRACT

The antileishmanial activity of valproic acid was evaluated in an *in vitro* culture of *Leishmania donovani* promastigotes using amphotericin B as standard. Both valproic acid and amphotericin B showed antileishmanial activity at IC₅₀s of 0.183 and 0.138 µg/ml, respectively. A homology model of *Leishmania donovani* histone deacetylase I (*Ld*HDACI) was built and validated using *in silico* tools. Docking valproic acid into the active site of this Zn-dependent *Ld*HDACI added a bidentate coordination to the tricoordinated metal. The resultant pentacoordinated Zn⁺² is no longer available for the natural substrate. Thus, the antileishmanial mechanism of valproic acid is thought to be via competitive inhibition of *Ld*HDACI.

Key Words: *Ld*HDAC1, leishmania, valproic acid, amphotericin B, histone deacetylase inhibitor, homology model, drug-repurposing.



INTRODUCTION

Leishmaniasis are group of clinically diverse vector-borne diseases, caused by a protozoa parasite of the genus *Leishmania*. There are three main forms of leishmaniasis, visceral, cutaneous and mucocutaneous [1]. Visceral leishmaniasis (VL) is the most life threatening form which if untreated is fatal. The disease is caused by *Leishmania donovani* complex in East Africa and Indian subcontinent and by *Leishmania infantum* in many parts of the world including Latin America and Mediterranean Basin [2]. VL affects 200 to 400 thousands people worldwide annually. Ninety percent of the VL occurs in Sudan, Ethiopia, Bangladesh, India, Nepal, and Brazil [3]. Currently, there is no available effective vaccine and on the other hand treatment of leishmaniasis

is based on pentavalent antimonials drugs and amphotericin B which are toxic and prone to drug resistance [4]. Therefore, it becomes mandatory to develop new drugs that would possibly be a key for safe, effective and affordable antileishmanial treatment. Drug development is tortuous, risky and financially burdensome with many compounds failing for every one that succeeds and reaches the market [5]. The application of known drugs to new indication, so-called drug-repurposing [6], has a significant advantage over traditional drug development. Having passed a significant number of toxicity studies and other tests, the repurposed drugs can bypass most of the early cost and time needed to bring a drug to a market. The identification of novel targets that interact with marketed drugs is the first step in assessing the repurposing potential [7].

*Corresponding Author Address: Magdi Awadalla Mohamed, PhD, Associate Professor Department of Pharmaceutical Chemistry, Faculty of Pharmacy, University of Khartoum, P. O. Box 1996, El Qasr Avenue, Khartoum 11111, Sudan; Email: mawadalla@uofk.edu

Cell proliferation and differentiation in protozoan parasites, like other eukaryotes, crucially depends on acetylation and deacetylation of histone and nonhistone proteins [8]. These transformations are catalyzed by histone acetyl transferases (HATs) and histone deacetylases (HDACs), respectively [9,10]. The genome of Leishmania parasite contains multiple genes that encode different HDACs which have been shown to be crucial for the survival and proliferation of the Leishmania parasite [11]. It was revealed that histone deacetylase inhibitors, specifically suberoylanilide hydroxamic acid (SAHA), trichostatin A (TSA), apicidin analogues and others have *in vitro* activity against *L. donovani* parasites [12,13]. This antiparasitic activity could be mediated by histone deacetylase inhibition [14]. The old anticonvulsant and mood stabilizer, valproic acid, has been found to inhibit both class I and II human HDACs, *Toxoplasma gondii* and *Schistosoma mansoni* HDACs [15–17]. We have recently reported the *in silico* activity of valproic acid against *Plasmodium falciparum* histone deacetylase 1 [18]. It was proposed that valproic acid would also have antileishmanial activity mediated through inhibition of *L. donovani* histone deacetylase I. The objective of this study was to investigate the *in vitro* activity of valproic acid against *Leishmania donovani* promastigotes. It was also hoped to propose a molecular mechanism for the expected antileishmanial activity of valproic acid using *in silico* tools.

MATERIALS AND METHODS

Drugs: Amphotericin B (Ambisome^(R)) was commercially purchased. Valproic acid (sodium salt, SUN Pharmaceutical Industries, India) was kindly provided by Azal Pharmaceutical Company, Sudan. The sodium valproate stock solution (20mg/ml; DMSO) was diluted two-fold with liver infusion treptose (LIT) complete media to obtain serial dilutions ranging from 200µg/ml to 0.049 µg/ml.

Parasite isolation and cultivation: A confirmed-positive VL patient was subjected to lymph node aspiration for parasite isolation. Biopsies were aseptically inoculated into vacutainers containing Novy-MacNeal-Nicolle (NNN) medium. Cultures were incubated at 25°C and parasite growth was monitored daily. Promastigotes were transferred into tissue culture flasks containing LIT media supplemented with 10% fetal calf serum (FCS), genatmycin and benzylpenicillin. The medium was changed every 3 days until promastigotes reached their stationary phase [19,20].

In vitro evaluation of antileishmanial activity: Promastigote density was adjusted to 2×10^6

parasites/ml using LIT complete media. A volume of 100 µl from parasite culture was transferred into 96-well flat bottom microtiter plate. Various concentrations of freshly prepared valproic acid solution were added (100µl) in triplicates. A negative control (DMSO without any drug), and positive control (amphotericin B) were treated similarly. The plates were incubated at 25°C for 72 hours. Parasites were counted by using hemocytometer [19,20].

Statistical analysis of data: Each experiment was performed in triplicates. Results were expressed as mean \pm standard deviation of the mean (SD) and analyzed using SPSS 18. The IC₅₀ values were calculated using GraphPad Prism 6.0 software.

Model building: The 430 amino acids sequence of *LdHDACI* (GI:193527475) was obtained from the NCBI protein database and YASARA structure program was used to build *LdHDACI* homology model [21]. The target sequence was PSI-BLASTed against UniRef90 and the resultant position-specific scoring matrix (PSSM) was used to search the PDB database for potential modeling templates. A prewritten macro was used to build different models based on the top five ranked templates. Finally, the best parts of the generated models were combined to obtain a hybrid model with better accuracy.

Model refinement: The hybrid model was further refined using YASARA short Molecular Dynamics (MD) simulation. The model refinement was conducted using YASARA2 force-field for 500 picoseconds at 298°K using the NVT canonical ensemble [22].

Model quality assessment: The MD simulated model's quality was assessed using online bioinformatics tools. Stereochemical accuracy and absolute quality were assessed using RAMPAGE and QMEAN online servers, respectively [23,24].

Molecular Docking: The 3D structure of valproic acid (CID: 3121) was obtained from the PubChem database. The ligand protonation state, energy minimization and molecular docking of valproic acid into *LdHDACI* were performed using MOE [25]. The plausible active site was identified using Alpha Site Finder. Valproic acid was docked into the identified active site using the triangle matcher placement method. Thirty docking poses were retained and scored using London *dG* scoring function. The retained poses were further refined to 0.1 kcal mol⁻¹ Å⁻¹ rms using CHARMM27 molecular mechanics force field [26] and rescored using the *dG* function.

RESULTS AND DISCUSSION

In vitro antileishmanial activity: Valproic acid, at dose range 200–0.05 µg/ml, showed 90.42±1.44–32.5±3.31% promastigote inhibitory activity. On the other hand, the standard antileishmanial drug amphotericin B showed 95.42±0.72–48.75±10.68% inhibitory activity at the same dose range (Table 1). The IC₅₀ values for valproic acid and amphotericin B were found to be 0.183 and 0.138 µg/ml, respectively (Figure 1). At 200 and 100 µg/ml, the inhibitory activity produced by valproic acid was significantly greater than that produced by amphotericin B at doses ≤ 1.56 µg/ml (One way ANOVA, P ≤ 0.05). Treatment of the *L. donovani* promastigotes with a mixture of the two drugs (1:1), at concentration ≥ 3.13 µg/ml, resulted in complete parasite growth inhibition. Further investigations are needed to develop a combination therapy of amphotericin B and valproic acid to increase the efficacy and reduce the dose and, thus, toxicity of each drug.

In silico study

Refined hybrid model: The hybrid model was found to be the best in terms of z-score (−0.967) and it was, therefore, further refined using YASARA2. The MD generated model with the lowest potential energy (−49946.70 kcal mol^{−1}) was employed for further work. This model adopted a canonical α/β HDAC fold similar to human and *Schistosoma mansoni* HDAC solved structures [27–29]. Similar to other HDACs, the model formed a single α/β domain composed of a central eight strands parallel β-sheet sandwiched by 16 α-helices (Figure 2). The model contained a divalent zinc ion at the bottom of the active site. The most important feature of the enzyme active site was the presence of HDACs canonical catalytic triad, where Zn²⁺ of the free enzyme formed coordinates with three amino acids, Asp190, His192 and Asp279 (Figure 2) [30].

Model quality assessment: RAMPAGE based-assessment of the refined model revealed that 97.2% of the amino acids were located in the favored region, 2.5% in allowed region, and the rest 0.3% residues were outliers (Figure 3). These findings greatly indicated that the stereochemical accuracy of the model is accepted in terms of dihedral angles (φ,ψ). On the other hand, the absolute quality of a model was evaluated by QMEAN server. Six descriptors of the model were combined and the resultant z-score was compared to scores of a non-redundant set of high resolution x-ray crystallography structures of similar size to the model's. The normalized QMEAN6 z-score for the model was within the standard deviation value typically obtained for crystallography structures

confirming that the model absolute quality was in match with them (Figure 4). With this model in hand, it was now time to conduct molecular docking of valproic acid to support the proposed *LdHDACI* inhibitory action.

Molecular docking: In Zn-dependent class I HDACs, the metal ion is coordinated at five points with a pentacoordinate geometry. It forms three coordinations with two Asp residues and one His in addition to two coordinations with a bidentate ligand [27–29]. In our ligand-free *LdHDACI* model, the metal forms three coordinates with Asp279, His192 and Asp190 (Figure 2). Docking valproic acid into the active site of *LdHDACI* expanded the coordination sphere to pentacoordinate by adding a bidentate coordination to Zn²⁺ via the carboxyl carbonyl oxygen and the hydroxyl oxygen of valproic acid (Figure 5). Thus, the pentacoordinated Zn²⁺ will not be available to interact with the natural substrate resulting in a competitive inhibition. Other interactions of valproic acid with the active site have also been identified. The amino acids Tyr318 and His154 formed hydrogen bonds with the carboxyl carbonyl oxygen and hydroxyl oxygen of valproic acid, respectively. Furthermore, the aliphatic parts of valproic acid showed hydrophobic interaction with Phe164. All these interactions are considered potential to increase the valproic acid affinity to *LdHDACI* active site. It is worth noting that, the well-known HDAC inhibitor trichostatin A (TSA) was reported to have a potent activity against *Leishmania donovani* [12]. However, its exact mechanism of action is not known. To support our proposed antileishmanial mechanism of valproic acid, we also docked TSA into *LdHDACI* active site. The same valproic acid's interactions were revealed by TSA, where it showed a bidentate interaction with Zn²⁺, hydrogen bonds with Tyr318 and His154, and hydrophobic interaction with Phe164 (Figure 5). Thus, the antileishmanial activity of valproic acid and TSA is very probably mediated through *LdHDACI* inhibition.

CONCLUSION

The well-known mood stabilizer and non-expensive valproic acid showed promising activity against *Leishmania donovani* promastigotes when compared to amphotericin B. *In silico* study revealed that this activity could be mediated through *LdHDACI* inhibition. Knowing that *LdHDACI* is crucial for the parasite throughout its life cycle [13], valproic acid could possibly be active against *Leishmania donovani* amastigotes. Further parasitological and efficacy studies should be conducted to confirm the *in vivo* antileishmanial efficacy of valproic acid.

ACKNOWLEDGMENT

The authors would like to thank Mr Abdelhafeiz M. Elsadig, Biomedical Research Centre, Ahfad

University for Women, Sudan, for excellent laboratory assistant.

Conflict of interest: The authors declare no conflict of interest.

Table 1: Antileishmanial activity of valproic acid against amphotericin B.

Concentration (µg/ml)	Mean %Inhibition ± SD	
	Valproic acid	Amphotericin B
200	90.42 ± 1.44 *↓	95.42 ± 0.72
100	85.83 ± 3.15 *↓	92.92 ± 0.72
50	83.33 ± 6.89	91.67 ± 4.39
25	75.42 ± 0.72 *↓	89.17 ± 0.72
12.5	60.00 ± 1.25 *↓	89.17 ± 3.15
6.25	61.67 ± 6.29 *↓	86.67 ± 5.64
3.13	64.17 ± 7.11 *↓	86.25 ± 2.17
1.56	57.50 ± 10.23 *↓	76.67 ± 4.02
0.78	62.08 ± 0.72 *↓	75.83 ± 4.02
0.39	51.25 ± 0.00 *↓	63.33 ± 4.39
0.20	36.67 ± 1.44	41.67 ± 5.05
0.10	39.58 ± 1.91	50.00 ± 7.50
0.05	32.50 ± 3.31	48.75 ± 10.68

↓* Significantly less potent compared to amphotericin B at the same dose (Student t-test, P ≤ 0.05).

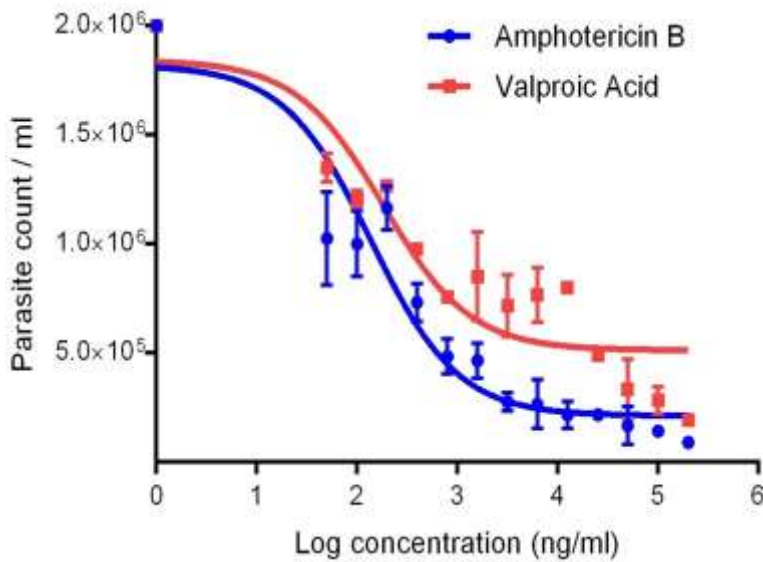


Figure 1. The viability of *L.donovani* promastigotes in the presence of different concentrations of valproic acid and amphotericin B.

The IC₅₀ is the antilogarithm of the concentration at which the curve passes through the 50% parasite count.

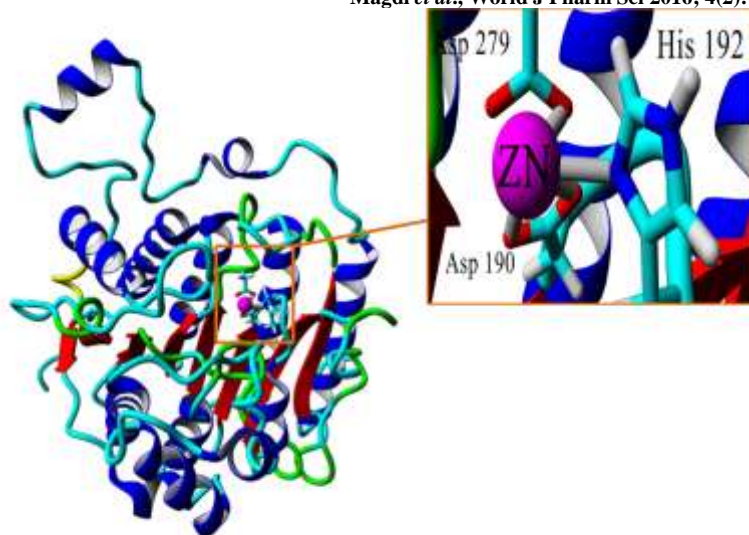


Figure 2. Ribbon representation of ligand-free *LdHDAC1* model.
The enlarged fragment shows zinc coordination state.

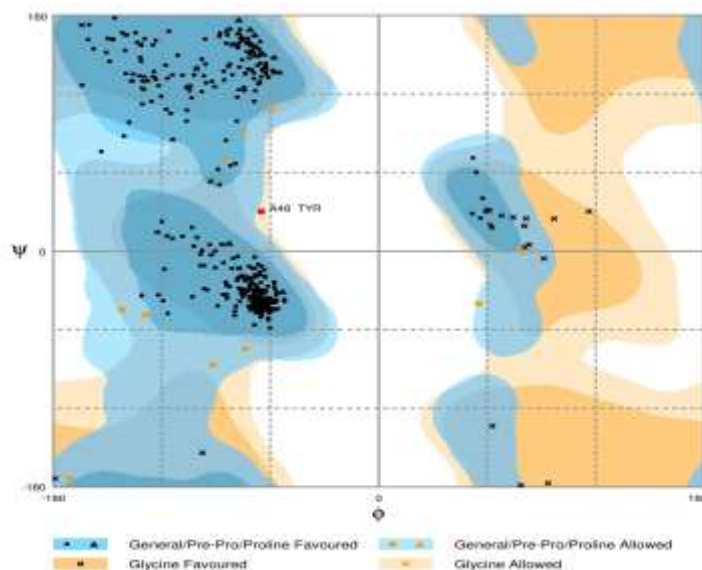


Figure 3. Ramachandran plot of dihedral angles (ϕ , ψ) of *LdHDAC1* model.

Number of residues in favoured region (~98.0% expected) : 386 (97.2%)

Number of residues in allowed region (~2.0% expected) : 10 (2.5%)

Number of residues in outlier region : 1 (0.3%)

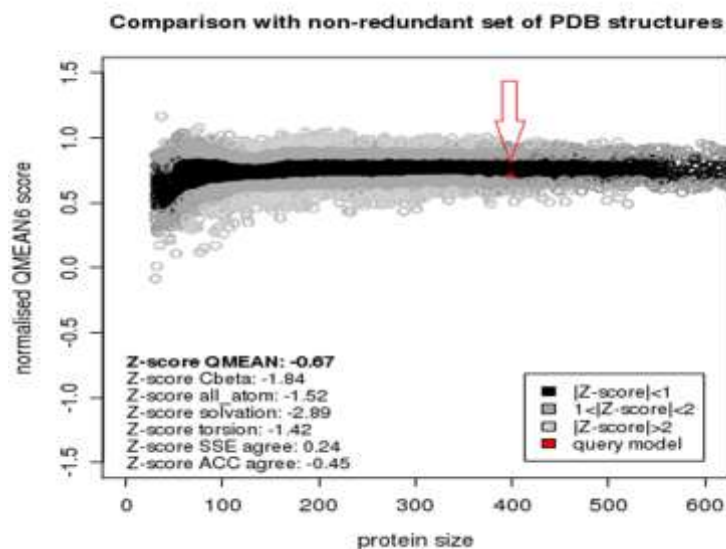


Figure 4. Normalized QMEAN6 z-score of *Ld*HDACI.
The red arrow highlights the position of the query model indicated by red 'X'.

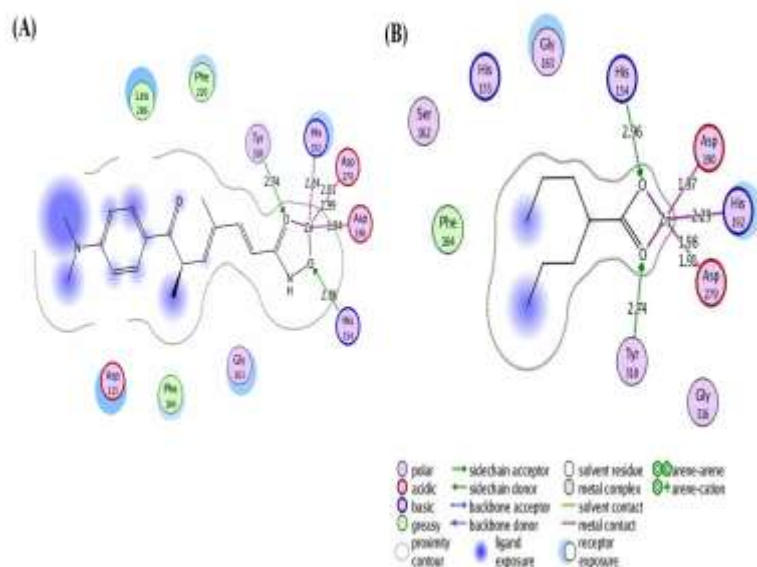


Figure 5. Ligand-model interactions.
A schematic diagram of *Ld*HDACI binding site showing the critical interactions undergone by (A) TSA and (B) valproic acid with zinc ion as well as the bonds' lengths.

REFERENCES

1. WHO | Leishmaniasis (n.d.). <http://www.who.int/mediacentre/factsheets/fs375/en/> (Accessed June 10, 2015).
2. Lukes J et al. Evolutionary and geographical history of the *Leishmania donovani* complex with a revision of current taxonomy. Proc Natl Acad Sci U S A 2007; 104(22): 9375–80.
3. Alvar J et al. Leishmaniasis worldwide and global estimates of its incidence. PLoS One 2012; 7(5): e35671.
4. Croft SL et al. Drug resistance in Leishmaniasis. Clin Microbiol Rev 2006; 19(1): 111–26.
5. DiMasi JA et al. The price of innovation: new estimates of drug development costs. J Health Econ 2003; 22(2): 151–85.
6. Sleigh SH, Barton CL. Repurposing strategies for therapeutics. Pharmaceut Med 2010; 24(3): 151–9. <http://link.springer.com/10.1007/BF03256811>. (Accessed September 15, 2015).

7. Oprea TI, Mestres J. Drug repurposing: far beyond new targets for old drugs. *AAPS J* 2012;14(4): 759–63.
8. Xu WS et al. Histone deacetylase inhibitors: molecular mechanisms of action. *Oncogene* 2007; 26(37): 5541–52. <http://www.ncbi.nlm.nih.gov/pubmed/17694093>. (Accessed May 3, 2014).
9. Ouaisi M, Ouaisi A. Histone deacetylase enzymes as potential drug targets in cancer and parasitic diseases. *J Biomed Biotechnol* 2006; ID 13474: 1–10.
10. Dokmanovic M, Marks PA. Prospects: histone deacetylase inhibitors. *J Cell Biochem* 2005; 96(2): 293–304. <http://www.ncbi.nlm.nih.gov/pubmed/16088937>. (Accessed May 3, 2014).
11. Khan SI et al. Antimalarial and antileishmanial activities of histone deacetylase inhibitors with triazole-linked cap group. *Bioorg Med Chem* 2011; 18(1): 1–33.
12. Hdac A et al. Antimalarial and antileishmanial activities of aroyl-pyrrolyl-hydroxyamides, a new class of histone deacetylase inhibitors. *Antimicrob Agents Chemother* 2004; 48(4): 1435–6.
13. Alonso VL, Serra EC. Lysine acetylation : elucidating the components of an emerging global signaling pathway in Trypanosomes. *J Biomed Biotechnol* 2012; ID 452934: 1–16.
14. Andrews KT et al. Potent antimalarial activity of histone deacetylase inhibitor analogues. *Antimicrob Agents Chemother* 2008; 52(4): 1454–61. <http://www.pubmedcentral.nih.gov/articlerender.fcgi?artid=2292526&tool=pmcentrez&rendertype=abstract>. (Accessed May 3, 2014).
15. Phiel CJ et al. Histone deacetylase is a direct target of valproic acid, a potent anticonvulsant, mood stabilizer, and teratogen. *J Biol Chem* 2001; 276(39): 36734–41.
16. Jones-Brando L et al. Drugs used in the treatment of schizophrenia and bipolar disorder inhibit the replication of *Toxoplasma gondii*. *Schizophr Res* 2003; 62(3): 237–44. [http://www.schres-journal.com/article/S0920-9964\(02\)00357-2/abstract](http://www.schres-journal.com/article/S0920-9964(02)00357-2/abstract). (Accessed January 04, 2016)
17. Azzi A et al. *Schistosoma mansoni*: developmental arrest of miracidia treated with histone deacetylase inhibitors. *Exp Parasitol* 2009; 121(3): 288–91. <http://www.sciencedirect.com/science/article/pii/S0014489408002968>. (Accessed January 04, 2016).
18. Elbadawi M et al. Valproic acid as a potential inhibitor of *Plasmodium falciparum* histone deacetylase 1 (*Pf*HDAC1): an in silico approach. *Int J Mol Sci* 2015; 16(2): 3915–31. <http://www.mdpi.com/1422-0067/16/2/3915/>. (Accessed October 06, 2015).
19. Saki J et al. In vitro antileishmanial activity of the medicinal plant - *Satureja khuzestanica* Jamzad. *J Med Plants Res* 2011; 5(24): 5912–15.
20. Hassan A et al. *Leishmania donovani* : an in vitro study of antimony-resistant amphotericin B-sensitive isolates. *Exp Parasitol* 2006; 114(4): 247–52.
21. Krieger E. Yet Another Scientific Artificial Reality Application 2004 (YASARA).
22. Krieger E et al. Improving physical realism, stereochemistry, and side-chain accuracy in homology modeling: Four approaches that performed well in CASP8. *Proteins-Structure Funct Genet* 2009; 77 (Suppl 9): 114–22.
23. Benkert P et al. QMEAN server for protein model quality estimation. *Nucleic Acids Res* 2009; 37: 510–14.
24. Lovell SC et al. Structure validation by C alpha geometry: phi,psi and C beta deviation. *Proteins-Structure Funct Genet* 2003; 50(3): 437–50.
25. Chemical Computing Group Inc. Molecular Operating Environment 2008 (MOE).
26. Mackerell AD et al. Extending the treatment of backbone energetics in protein force fields: limitations of gas-phase quantum mechanics in reproducing protein conformational distributions in molecular dynamics simulations. *J Comput Chem* 2004; 25(11): 1400–15.
27. Bressi JC et al. Exploration of the HDAC2 foot pocket: synthesis and SAR of substituted N-(2-aminophenyl)benzamides. *Bioorganic Med Chem Lett* 2010; 20(10): 3142–45.
28. Bürli RW et al. Design, synthesis, and biological evaluation of potent and selective class IIa histone deacetylase (HDAC) inhibitors as a potential therapy for huntington’s disease. *J Med Chem* 2013; 56(24): 9934–54.
29. Marek M et al. Structural basis for the inhibition of histone deacetylase 8 (HDAC8), a key epigenetic player in the blood fluke *Schistosoma mansoni*. *PLoS Pathog* 2013; 9(9): e1003645.
30. Lombardi PM et al. Structure, mechanism, and inhibition of histone deacetylases and related metalloenzymes. *Curr Opin Struct Biol* 2011; 21(6): 735–43.